Noncanonical MicroRNA (miRNA) Biogenesis Gives Rise to Retroviral Mimics of Lymphoproliferative and Immunosuppressive Host miRNAs

Rodney P. Kincaid,[a] Yating Chen,[a] Jennifer E. Cox,[a] Axel Rethwilm,[b] Christopher S. Sullivan[a]

The University of Texas at Austin, Molecular Biosciences, Austin, Texas, USA[a]; Institut für Virologie und Immunbiologie, Universität Würzburg, Würzburg, Germany[b]

ABSTRACT **MicroRNAs (miRNAs) play regulatory roles in diverse processes in both eukaryotic hosts and their viruses, yet fundamental questions remain about which viruses code for miRNAs and the functions that they serve. Simian foamy viruses (SFVs) of Old World monkeys and apes can zoonotically infect humans and, by ill-defined mechanisms, take up lifelong infections in their hosts. Here, we report that SFVs encode multiple miRNAs via a noncanonical mode of biogenesis. The primary SFV miRNA transcripts (pri-miRNAs) are transcribed by RNA polymerase III (RNAP III) and take multiple forms, including some that are cleaved by Drosha. However, these miRNAs are generated in a context-dependent fashion, as longer RNAP II transcripts spanning this region are resistant to Drosha cleavage. This suggests that the virus may avoid any fitness penalty that could be associated with viral genome/transcript cleavage. Two SFV miRNAs share sequence similarity and functionality with notable host miRNAs, the lymphoproliferative miRNA miR-155 and the innate immunity suppressor miR-132. These results have important implications regarding foamy virus biology, viral miRNAs, and the development of retroviral-based vectors.**

IMPORTANCE **Fundamental questions remain about which viruses encode miRNAs and their associated functions. Currently, few natural viruses with RNA genomes have been reported to encode miRNAs. Simian foamy viruses are retroviruses that are prevalent in nonhuman host populations, and some can zoonotically infect humans who hunt primates or work as animal caretakers. We identify a cluster of miRNAs encoded by SFV. Characterization of these miRNAs reveals evolutionarily conserved, unconventional mechanisms to generate small RNAs. Several SFV miRNAs share sequence similarity and functionality with host miRNAs, including the oncogenic miRNA miR-155 and innate immunity suppressor miR-132. Strikingly, unrelated herpesviruses also tap into one or both of these same regulatory pathways, implying relevance to a broad range of viruses. These findings provide new insights with respect to foamy virus biology and vectorology.**

Received 17 January 2014 **Accepted** 12 March 2014 **Published** 8 April 2014

Citation Kincaid RP, Chen Y, Cox JE, Rethwilm A, Sullivan CS. 2014. Noncanonical microRNA (miRNA) biogenesis gives rise to retroviral mimics of lymphoproliferative and immunosuppressive host miRNAs. mBio 5(2):e00074-14. doi:10.1128/mBio.00074-14.

Editor Vincent Racaniello, Columbia University College of Physicians & Surgeons

Address correspondence to Christopher S. Sullivan, Chris_sullivan@mail.utexas.edu.

Simian foamy viruses (SFVs) are complex retroviruses belonging to the family *Spumaretrovirinae* that infect a variety of primate hosts (1). Although endemic infection of human populations by FVs has not been observed, zoonotic transmission of SFVs to humans may occur through hunting and butchering of some nonhuman primates, as well as through injuries sustained by caregivers in zoos and animal research facilities (2–7). SFVs do not currently have disease associations in the context of infections endemic to primates or zoonotic human infections, yet they are capable of establishing long-term persistent infections (8, 9). However, a complete mechanistic understanding of how SFVs are able to evade the host immune response and maintain long-term infections is lacking.

microRNAs (miRNAs) are small regulatory RNAs encoded by most eukaryotes and some viruses (reviewed in references 10–13). Diverse viruses have been shown to encode miRNAs, but the extent to which different virus families utilize miRNAs remains a fundamental question. Furthermore, the functions of the majority of viral miRNAs are unknown. However, several themes are emerging from the currently available data, including optimization of productive versus latent infection, immune evasion, and promotion of host cell viability (11, 14). Some viral miRNAs have been reported to achieve their functions by tapping into host regulatory networks by mimicking host miRNAs through partial sequence similarity (10).

We have improved a combined computational and synthetic approach to predict miRNA genes from primary sequence information and applied it to the foamy viruses (15). This analysis identified clusters of candidate RNA polymerase III (RNAP III)-transcribed miRNA genes in the long terminal repeats (LTRs) of SFVs and some FVs with nonprimate hosts. We characterized miRNAs of the African green monkey FV (SFVagm). These miRNAs are generated from atypical RNAP III primary transcripts. Two of the SFVagm miRNAs share seed identity and functionality with host miRNAs miR-132 and miR-155. The relevance of these findings to FV biology and vectorology is discussed.

RESULTS

FVs encode miRNAs. Using a combined computational and synthetic approach, we previously reported the identification and

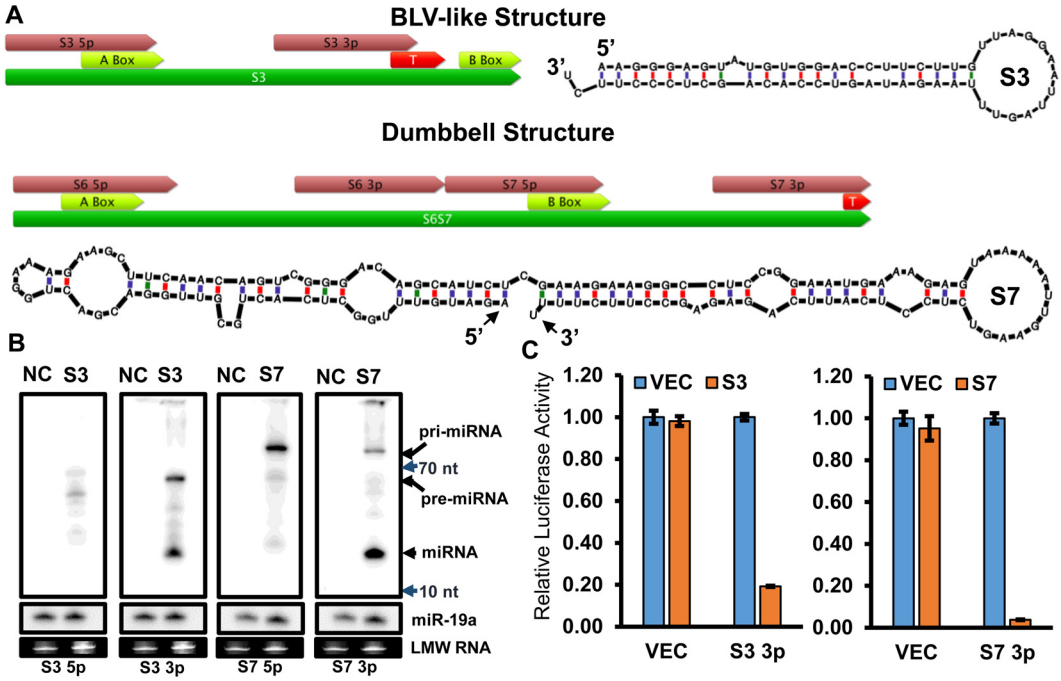

FIG 1 A combined computational and synthetic approach identifies SFV-encoded candidate miRNAs. (A) Diagram of predicted genetic structure and secondary structure predictions by Mfold for two candidate miRNAs from SFVagm. Termini in diagrams have been updated to start and termination sites from the following RNA-seq data. Mauve arrows indicate the most abundantly mapped small RNAs from RNA-seq data (Fig. 2). Yellow arrows indicate predicted RNAP III promoter elements. Red arrows indicate predicted RNAP III terminator sequences. (B) Northern blot analysis of total RNA extracted from HEK293T cells transfected with either negative-control empty expression vector (NC) or the indicated synthetic gene (S3, S7) constructs. Ethidium bromide-stained low-molecular-weight (LMW) RNA is provided as a loading control. Blots were also probed for hsa-miR-19a as an additional control. nt, nucleotides. (C) RISC reporter assays for synthetic miRNA candidate constructs. HEK293T cells were cotransfected with either empty expression vector (VEC) or the indicated synthetic gene construct and both control firefly luciferase reporter and *Renilla* luciferase reporter plasmids with vector UTR (VEC) or two sites perfectly complementary to the indicated predicted miRNA arm (S3 3p or S7 3p). The mean relative luciferase activity ratios, normalized to the results for the control *Renilla* luciferase vector 3′ UTR, are graphed. Error bars represent the standard deviations (SD) of three replicates.

characterization of viral miRNAs encoded by a deltaretrovirus, bovine leukemia virus (BLV) (15). We have subsequently modified our algorithmic approach to include new features derived from the BLV miRNAs. These features include searching for an RNAP III terminator sequence at the 3′ base of predicted RNA stem-loop structures and modification of the RNAP III promoter sequences to include noncanonical A and B box sequences from the BLV miRNAs. The new approach identified additional predicted miRNA candidates (see Data Set S1 in the supplemental material). Two candidates from simian foamy virus of African green monkey (SFVagm), two from simian foamy virus of rhesus macaque (SFVmac), and one from feline foamy virus (FFV) were chosen for further screening (Fig. 1A; see Fig. S1 in the supplemental material). The candidate miRNA sequences were synthesized in the context of minimal bacterial plasmids. HEK293T cells were transfected with these plasmids, and Northern blot analysis was performed. This analysis revealed readily detectable banding patterns consistent with the predicted primary (pri-), pre-, and mature miRNAs (Fig. 1B; Fig. S1). Luciferase-based reporters were used to test whether the observed small RNAs generated from the SFVagm constructs were active in the RNA-induced silencing complex (RISC). Cotransfection of these reporters with the synthetic miRNA plasmids resulted in significant and specific inhibition of reporter activity, indicating that the putative miRNAs are active in RISC (Fig. 1C).

Next, we investigated whether the miRNAs are expressed in the context of SFVagm infection. RNA profiling was conducted on small RNA fractions extracted from HeLa cells 3 days after infection with SFVagm (Fig. 2; see Table S1 in the supplemental material). This analysis confirmed the expression of the computationally predicted miRNAs, as well as additional viral miRNA candidates in the U3 LTR region. Importantly, the read patterns mapping to the SFVagm genome displayed the hallmarks of *bona fide* miRNAs, including a predominant size of ~22 nucleotides (Fig. S2A) and mapping to predicted RNA stem-loop secondary structures with guide strand/passenger strand complementarity offset typically by 3′ overhangs, a hallmark of RNase III-like enzymatic processing (Fig. S2B). As an additional verification of the RNA-seq-mapped small RNAs, Northern blot analysis was conducted for each of the abundantly mapped candidates (Fig. S3). This analysis revealed readily detectable small RNAs corresponding mostly to the abundant products identified by small RNA sequencing. However, we note that for some pre-miRNAs, such as SFVagm-miR-S3, the 5p- and 3p-derived miRNAs showed inverse abundance in the Northern or RNA-seq analyses (Fig. 2; Fig. S3). We speculate that this is due to inherent sequence biases in the RNA-seq library construction. In addition, banding patterns indicating the detection of some longer transcripts are consistent with the predicted gene architectures. Comparison of the SFVagm miRNA sequences with those of human miRNAs revealed several with similarity in the miRNA seed region (Table S2). The seed region encompasses nucleotides 2 to 7 of the miRNA and is an

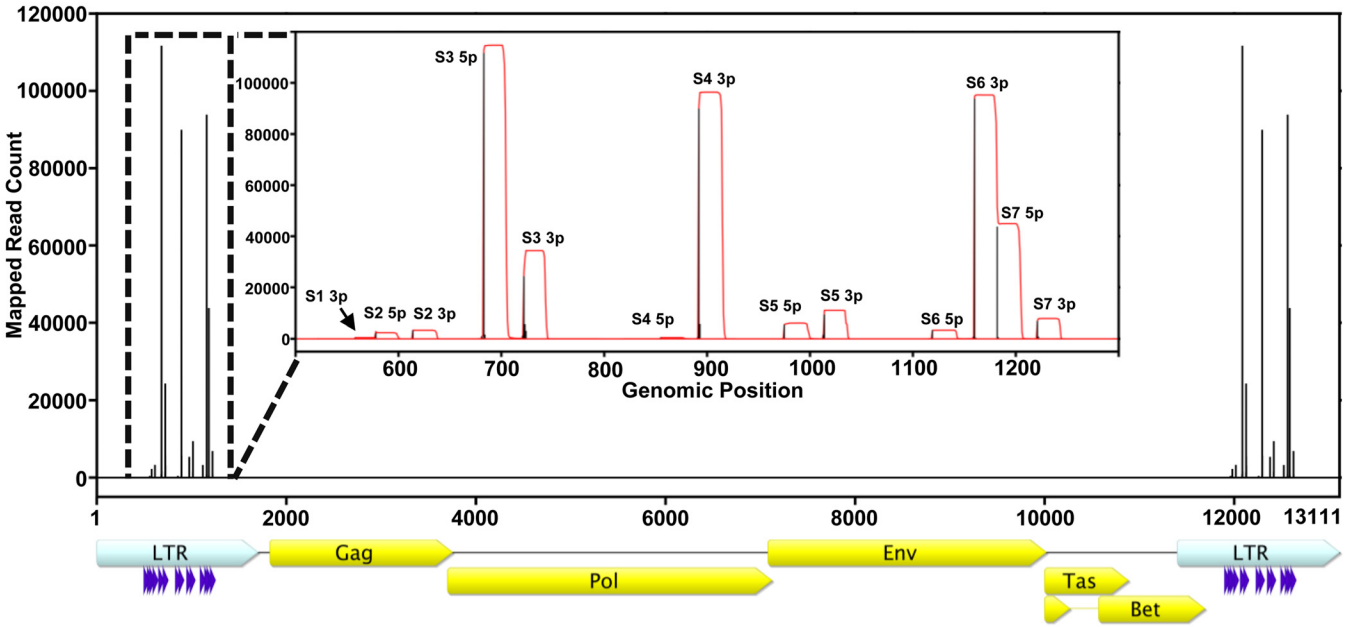

FIG 2 Small RNA profiling of SFVagm-infected cells reveals a cluster of miRNA candidates in the SFVagm LTR. RNA-seq analysis was performed on size-fractionated RNA extracted from HeLa cells 72 h after infection with SFVagm. The horizontal axis indicates the genomic position relative to the SFVagm reference genome (NC_010820). The vertical axis indicates the mapped small RNA read count (black impulses indicate start counts of RNA reads). An SFVagm genomic organization map based on annotation in reference sequence NC_010820 is provided below the horizontal axis. Light-blue arrows indicate LTR regions, yellow arrows indicated protein coding sequences, and dark blue arrows indicate the mapped small RNAs. Inset graph displays an enlargement of the LTR region to provide finer detail of the candidate miRNA cluster (black impulses indicate start counts of RNA reads and red lines indicate overall coverage).

important determinant of canonical miRNA target interaction (16). Therefore, we chose to focus our investigation on the candidate miRNAs SFVagm-miR-S4 and SFVagm-miR-S6.

Noncanonical biogenesis of SFV miRNAs. We tested our original prediction of RNAP III-dependent transcription of the primary miRNA transcripts (pri-miRNA). The banding patterns detected via Northern blot analysis (Fig. 1B; see Fig. S1 and Fig. S3 in the supplemental material) and the fact that several of the SFV miRNAs end in a stretch of Us (RNAP III terminator sequence) (Fig. S2B) were consistent with RNAP III-mediated transcription. We used a strategy in which plasmids containing the miRNA and flanking sequences are transfected into HEK293T cells, followed by treatment with α-amanitin at a concentration known to inhibit RNAP II transcription but not RNAP III transcription (17). For controls, we utilized two characterized viral noncoding RNAs (ncRNAs), the RNAP II-dependent HSUR4 from herpesvirus saimiri and the RNAP III-dependent MHV68-miR-M1-7 from mouse gammaherpesvirus 68 (17, 18). Northern blot analysis revealed that α-amanitin treatment strongly inhibited the expression of HSUR4 but not MHV68-miR-M1-7 or any of the tested SFV miRNAs (Fig. 3A). These results combined with our initial observations are consistent with the SFV miRNAs being transcribed by RNAP III.

Most host miRNAs are processed from longer primary miRNA transcripts into smaller pre-miRNA stem-loop structures by the Microprocessor complex (19). However, the reported BLV and MHV68 RNAP III-transcribed miRNAs are not processed by Drosha, the endonuclease component of Microprocessor (15, 17). Some of the SFV candidate miRNAs have predicted BLV miRNA-like precursor structures and gene architecture (Fig. 1A; see Fig. S1B in the supplemental material). However, others produced an additional, slower-migrating band by Northern analysis that is consistent with the predicted longer primary transcript containing up to two pre-miRNA-like structures (Fig. 1A and B; Fig. S1A and S3). To test whether the SFVagm-miR-S4 and SFVagm-miR-S6 pri-miRNAs are processed by Drosha, we performed small interfering RNA (siRNA) knockdown of Drosha in HEK293T cells, followed by transfection of viral miRNA vectors and Northern blot analysis (Fig. 3B). For controls, we included the Drosha-dependent SV40-miR-S1 from simian virus 40 and the Drosha-independent MHV68-miR-M1-7. As expected, Drosha knockdown resulted in decreased SV40-miR-S1 pre-miRNA and no significant change in MHV68-miR-M1-7 pre-miRNA. Unlike other known viral pol III miRNAs, the tested SFV miRNAs exhibited decreased pre-miRNA levels upon Drosha knockdown. Next, we tested the effects of overexpression of Drosha and its binding partner DGCR8. HEK293T cells were sequentially transfected first with Drosha/DGCR8 and then with miRNA expression vectors, followed by Northern blot analysis (Fig. 3C). As expected, Drosha/DGCR8 overexpression resulted in an increase in SV40-miR-S1 pre-miRNA and no noticeable change in MHV68-miR-M1-7 pre-miRNA. However, consistent with our Drosha knockdown experiments described above, the overexpression of Drosha/DGCR8 resulted in increased SFV pre-miRNA. These data are consistent with Drosha-dependent production of these SFV pre-miRNAs from longer RNAP III transcripts.

Since the genomic region encoding the SFV miRNAs is also transcribed by RNAP II to generate viral genomic RNA and mRNAs, we next tested the ability of Drosha to cleave SFV pri-miRNAs in the context of longer RNAP II transcripts. To accomplish this, we utilized a Drosha cleavage efficiency assay that has been previously described (15). SFV pri-miRNA sequences and

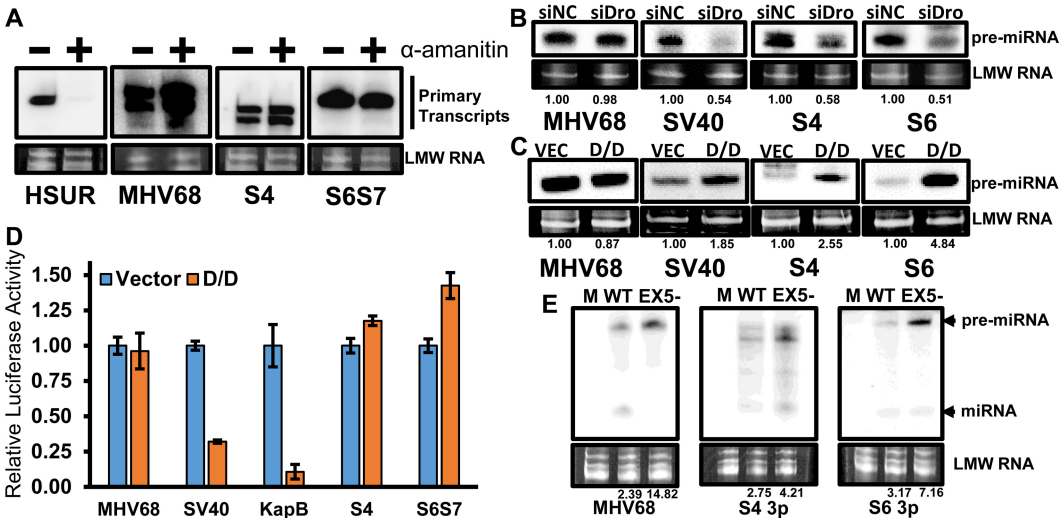

FIG 3 Characterization of SFV miRNA biogenesis reveals noncanonical mechanisms. (A) Northern blot analysis of total RNA extracted from HEK293T cells transfected with the indicated miRNA expression vectors and either treated or not treated with the RNAP II inhibitor α-amanitin as indicated. Ethidium bromide-stained LMW RNA is provided as a loading control. (B) Northern blot analysis of total RNA extracted from HEK293T cells transfected with the indicated miRNA expression vectors and Drosha siRNA (siDro) or negative-control siRNA (siNC). Numbers below lanes indicate signal intensity of pre-miRNA relative to siNC lane for each expression vector. Ethidium bromide-stained low-molecular-weight RNA is provided as a loading control. (C) Northern blot analysis of total RNA extracted from HEK293T cells cotransfected with the indicated miRNA expression vectors and either Drosha/DGCR8 expression vectors (D/D) or empty vector (VEC). Numbers below lanes indicate signal intensity of pre-miRNA relative to VEC lane for each expression vector. Ethidium bromide-stained LMW RNA is provided as a loading control. (D) Drosha cleavage assay was performed on FV miRNA candidates and control miRNAs cloned into the 3′ UTR of *Renilla* luciferase vectors. The indicated miRNA 3′ UTR vectors were cotransfected with control firefly luciferase vector and either Drosha/DGCR8 expression vectors (D/D) or empty vector (Vector). The mean relative luciferase activity ratios, normalized to the results for the control vector *Renilla* luciferase vector 3′ UTR, are graphed. Error bars represent the SD of three replicates, and the *P* values were calculated using Student's *t* test. (E) Northern blot analysis of total RNA extracted from untransfected DLD1 (M), wild-type DLD1 (WT), or DLD1 DicerEx $5^{-/-}$ hypomorph (EX5-) cells transfected with the indicated miRNA expression vectors. Numbers below lanes indicate pre-miRNA signal divided by mature miRNA signal. Ethidium bromide-stained LMW RNA is provided as a loading control.

control pri-miRNA sequences were cloned into the 3′ untranslated region (UTR) of *Renilla* luciferase reporters. These vectors were cotransfected with control firefly luciferase reporter and either Drosha/DGCR8 expression vectors or empty vector, and dual-luciferase assays were performed (Fig. 3D). As expected, overexpression of Drosha/DGCR8 resulted in significant reduction of the relative luciferase activity for the Drosha-dependent control reporters (SV40-miR-S1 and KapB), while no significant difference was observed for the Drosha-independent MHV68-miR-M1-7 reporter. Remarkably, none of the tested FV pri-miRNA constructs exhibited a decrease with Drosha/DGCR8 overexpression. These results suggest that the SFV miRNAs assayed are not efficiently processed in the context of longer RNAP II-transcribed RNAs.

Dicer is the enzyme that cleaves pre-miRNAs into mature miRNA duplexes in the canonical miRNA biogenesis pathway. To determine whether the SFV miRNAs were processed by the host enzyme Dicer, DLD1 Dicer-hypomorphic cells (20) and parental DLD1 wild-type cells were transfected with miRNA expression vectors and Northern blot analysis was performed (Fig. 3E). The Dicer-dependent control, MHV68-miR-M1-7, showed an increased ratio of the pre-miRNA to mature miRNA. Similar ratio changes were observed for the SFV miRNA constructs tested. These data support Dicer-dependent processing of the SFV miRNAs assayed.

To dissect the genetic elements of an SFV miRNA gene, a series of mutations were made in the predicted promoter and terminator elements of SFVagm-miR-S4 (see Fig. S4A in the supplemental material). These constructs were transfected into HEK293T cells, and total RNA was extracted and assayed by Northern blotting (Fig. S4B). As predicted, disruption of either the A box or B box promoter elements resulted in decreased expression, while disruption of the terminator sequence resulted in slower-migrating bands, consistent with read-through transcription to downstream terminator-like sequences. It is worth noting that longer read-through transcripts are not processed into mature miRNA sequences. Combined with the Drosha cleavage assay described above (Fig. 3D), these data are consistent with SFV miRNAs not being processed in the context of longer transcripts.

Functions of SFV miRNAs. Several other viruses, including herpesviruses and the retrovirus BLV, have been shown to mimic host miRNAs through seed similarity (reviewed in reference 11). The SFVagm-encoded miR-S4-3p shares seed identity with host miRNA miR-155 (Fig. 4A). This is notable because miR-155 is associated with cell survival and lymphoproliferation and at least three other herpesviruses encode analogs of this miRNA or induce its expression (21–26). Furthermore, candidate miR-S6-3p shares seed identity with the host miRNA family miR-132/212 (Fig. 4A), which has been shown to be a negative regulator of innate immunity that is induced by Kaposi's sarcoma-associated herpesvirus (KSHV) infection (27).

We first confirmed that these SFV miRNAs are active in RISC (Fig. 4B). As expected, luciferase reporters bearing perfectly complementary sequences in their 3′ UTRs were specifically and robustly downregulated when cotransfected with the respective FV miRNA expression vector. Next, to test whether the SFVagm miR-

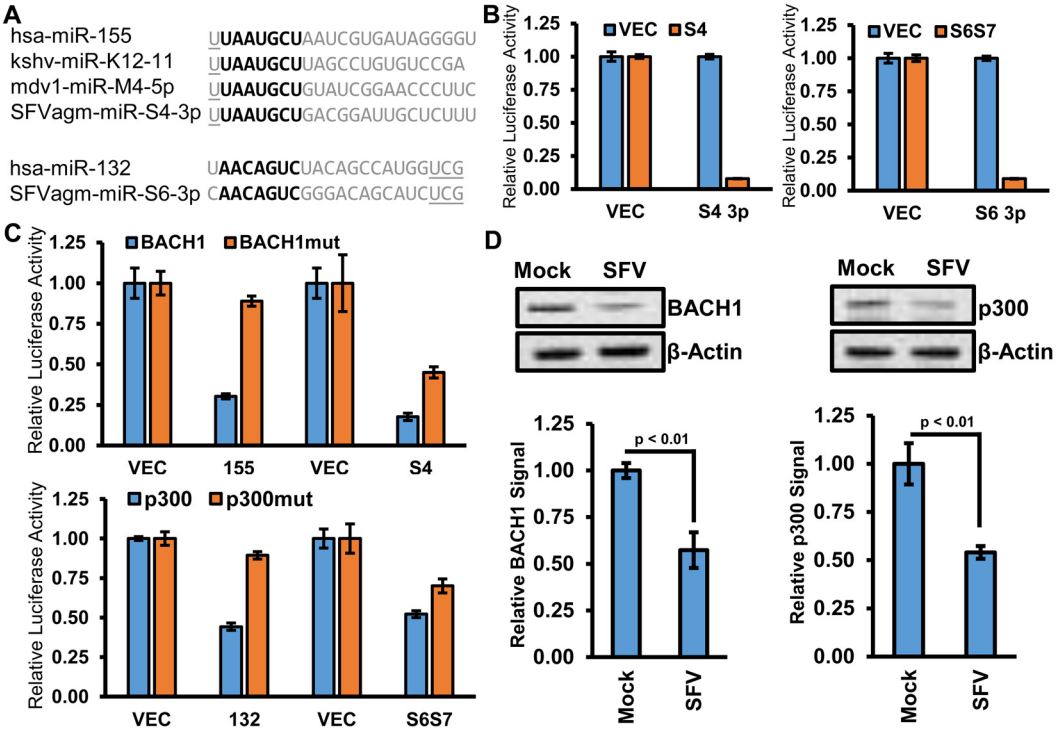

FIG 4 Some SFV-encoded miRNAs function as analogs of host miRNAs. (A) Sequence comparison of SFV miRNAs SFVagm-miR-S4-3p and SFVagm-miR-S6-3p to miRNAs hsa-miR-155 and hsa-miR-132, respectively. The miRNA seed sequence is indicated in bold. (B) RISC reporter assays for SFVagm miRNA candidates. HEK293T cells were cotransfected with either empty expression vector (VEC) or the indicated synthetic gene construct and both control firefly luciferase reporter and *Renilla* luciferase reporter plasmids with vector UTR (VEC) or two sites perfectly complementary to the indicated predicted miRNA arm (S4 3p or S6 3p). The mean relative luciferase activity ratios, normalized to the results for the control vector *Renilla* luciferase vector 3′ UTR, are graphed. Error bars represent the SD of three replicates. (C) BACH1 and p300 3′ UTR reporter assays were performed. HEK293T cells were cotransfected with either empty expression vector (VEC) or the indicated synthetic gene construct and the indicated 3′ UTR reporter. The pGL3-based BACH1 reporters and empty vector controls included cotransfection of pcDNA3.1dsLuc2CP control vector. The psiCheck2-based p300 reporters express both firefly and *Renilla* luciferase from the same plasmid. The BACH1mut and p300mut vectors contain mutations in seed regions complementary to miR-155 and miR-132, respectively (26, 27). The mean relative luciferase activity ratios, normalized to the results for the VEC control *Renilla* luciferase vector, are graphed. Error bars indicate SD. (D) Immunoblot analysis of protein extracted from HEK293 cells 72 h after infection with SFV or mock infection (Mock). A representative blot for each indicated target (BACH1 or p300) is provided, along with a blot for β-actin as a loading control. Graphs represent quantification of the means of three independent replicates relative to data for mock-infected cells. Error bars indicate SD, and *P* values were calculated with Student's *t* test.

NAs could target transcripts that were similar to the host miRNAs, we used previously reported luciferase 3′ UTR reporters for an miR-155 target, BACH1 (26), and an miR-132 target, p300 (27). Reporter vectors were cotransfected with miRNA expression vectors, and dual-luciferase assays were performed (Fig. 4C). The FV miRNAs significantly inhibited the relative luciferase activities for the respective reporters. Similar to their host counterparts, this regulation was specific, since the mutant reporters (containing small disruptions in the seed-complementary regions of each respective 3′ UTR) reduced the viral miRNA-mediated regulation that we observed. We next assayed protein levels by Western blotting in HEK293 cells infected with SFVagm (Fig. 4D). The protein levels of both BACH1 and p300 were significantly reduced (>40%) in cells infected with SFVagm. Although non-miRNA factors related to viral infection likely contributed to the observed effects, these data are consistent with direct targeting, as observed in the reporter assays. Therefore, we conclude that SFVagm-miR-S4 can function as an analog of host miRNA miR-155 and SFVagm-miR-S6 can function as an analog of host miRNA miR-132.

Host miR-132 has been identified as having a role in the down-regulation of p300, which is a transcriptional coactivator of the type I interferon (IFN) response (27, 28). To determine whether miR-S6 (the viral miR-132 seed mimic) shares this functionality, we first tested miR-S6 for the ability to alter IFN-mediated transactivation of an interferon-stimulated response element (ISRE)-driven luciferase reporter. HEK239T cells were cotransfected with either miR-S6 expression vector or positive-control (miR-132 [27] and miR-122 [29]) or negative-control (empty) vectors and then treated with universal type I interferon. As previously published (27, 29), both positive controls reduced ISRE activity. Importantly, the expression of miR-S6 resulted in a decrease in ISRE activity comparable to the effects of the positive controls (Fig. 5A). Next, we used a more biological assay to further determine the functionality of miR-S6 in regulating the IFN response. Stable B-cell lines were generated that expressed positive-control (miR-132) or negative-control (irrelevant Epstein-Barr virus [EBV] miRNA EBV-miR-BART4 or empty lentivector) miRNAs or miR-S6. Then, the growth rates of all the cell lines in either the presence or absence of exogenously added universal type I interferon were measured. All the cell lines grew similarly in the absence of interferon (Fig. 5B). However, as we previously demonstrated (30), treatment with IFN significantly reduced the growth rates of the vector and irrelevant-miRNA-expressing cell lines. In contrast,

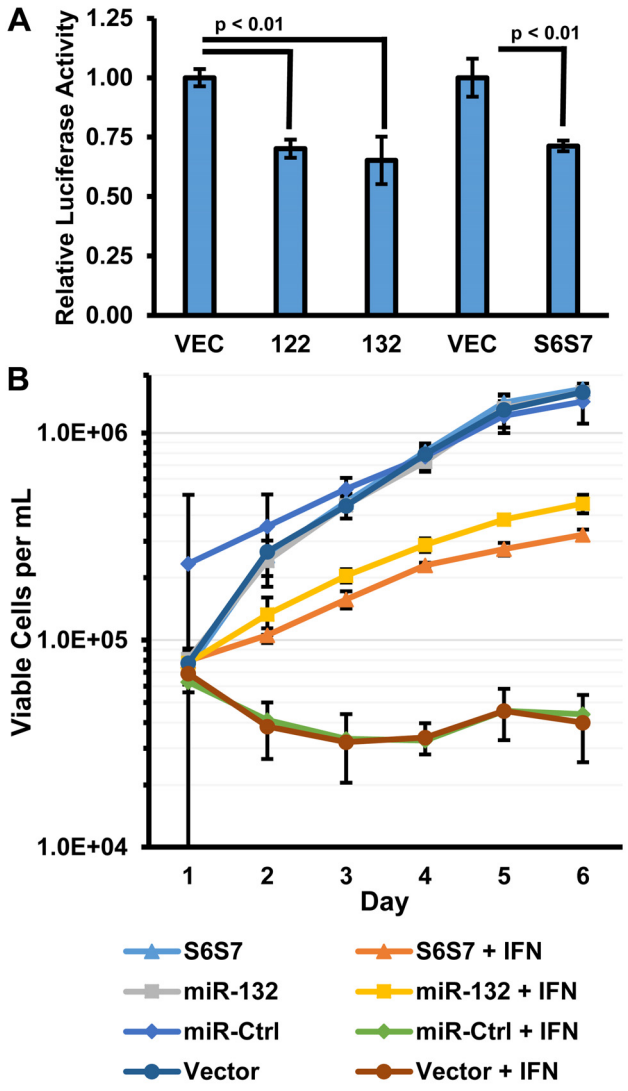

FIG 5 SFVagm-miR-S6 mimics host miR-132 in inhibition of the IFN (interferon) response. (A) HEK293T cells were cotransfected with plasmids expressing an IFN-responsive firefly luciferase reporter, a transfection control expressing *Renilla* luciferase from a constitutive promoter, and either an miRNA expression plasmid (miR-122, miR-132,or S6S7) or control empty vector (VEC). Forty-eight hours after transfection, cells were treated with 100 U/ml universal type I IFN. Twelve hours later, a dual-luciferase assay was performed. Relative luciferase activity is normalized to the respective vector control. The means are graphed along with error bars that represent the SD of three replicates, and *P* values were calculated with Student's *t* test. (B) Stable B-cell lines expressing miR-132, EBV-miR-BART4 (miR-Ctrl), SFVagm-miR-S6 (S6S7), or empty vector (Vector) were treated daily with 250 U/ml of interferon (+ IFN) or BSA, and viable cells (as assayed by trypan blue staining) were counted. For all experiments, the means of three independent biological replicates are shown and error bars indicate SD.

both the miR-S6- and host miR-132-expressing cells had substantial increases in viable cell counts compared to the viable cell counts in the control cell lines (up to 8- and 11-fold, respectively). These results indicate that both miR-132 and miR-S6 can provide a growth advantage to B cells that are exposed to interferon. Combined, our data show that SFVagm-miR-S6 is a functional mimic of the IFN-suppressive host miRNA miR-132.

DISCUSSION

Over 300 viral miRNAs have been reported (31), and the complete list of viral families that encode them remains a work in progress. We have previously reported that the deltaretrovirus BLV encodes a cluster of RNAP III-transcribed miRNAs (15), and these miRNAs were shown to be made *in vivo* (32). Using a refined computational and synthetic strategy, we identified candidate miRNAs in FVs that share predicted promoter architecture similar to that of BLV miRNAs, as well as a more canonical ordering of predicted promoter and terminator elements (Fig. 1A; see Fig. S1 in the supplemental material). Small RNA profiling of SFVagm-infected cells confirmed our initial predictions and revealed additional candidate miRNAs located in a cluster mapping to the LTR region (Fig. 2). Thus, our work adds to the modest but increasing number of viruses with RNA genomes known to make miRNAs.

Probing the pathways that give rise to the SFV miRNAs revealed noncanonical biogenesis strategies, including longer RNAP III transcripts which give rise to pre-miRNAs in a Drosha-dependent manner (Fig. 3B and C). This was unanticipated, as these pri-miRNAs are not predicted to have a canonical "base" region that has long been associated with Microprocessor-mediated cleavage (33, 34). Importantly, we provide evidence suggesting that the processing of these SFV miRNAs is context dependent, as longer RNAP II transcripts that span the miRNAs are immune to Microprocessor activity and disruption of a terminator sequence resulted in longer transcripts but undetectable miRNA production (Fig. 3D; see Fig. S4 and S5 in the supplemental material). In this way, FVs may avoid fitness costs associated with cleavage of genomic or mRNA transcripts. Future mechanistic studies will be needed to determine why extended transcripts are not efficiently processed and whether they are dependent on other enzymes for their maturation. Additionally, the shorter FV pri-miRNAs (e.g., SFVagm-miR-S3) resemble the Drosha-independent BLV pri-miRNAs in predicted structure, but it awaits experimental confirmation whether this class of FV miRNAs is also generated via a Drosha-independent mechanism. Thus, FV transcripts represent an arena ripe for future efforts to better understand Microprocessor pri-miRNA recognition and processing.

Our bioinformatics results predict that similar miRNA genes are shared among other SFVs, including the prototype foamy virus (PFV), as well as some nonprimate FVs (see Data Set S1 in the supplemental material). Our predictions identified candidate BLV-like miRNA genes in the feline FVs and candidate longer miRNA genes in the bovine and equine FVs (Data Set S1). Although our initial tests of a predicted FFV miRNA (Fig. S1B) were positive, these results should only be considered provisional until they are further validated in infected cells. However, while our paper was under review, Whisnant et al. (35) reported miRNAs encoded by the bovine foamy virus, suggesting shared atypical biogenesis of some miRNAs from diverse FVs. Combined, these observations imply that this mode of miRNA production may be of deep evolutionary origin.

We observed similarities between the SFV miRNAs and host miRNA families (see Table S2 in the supplemental material). One of the most striking observations was that SFVagm-miR-S4-3p shares seed identity and functionality with host miR-155, a noted host oncogenic miRNA (oncomiR) (36, 37) (Fig. 4). At least two other viruses, Marek's disease virus type 1 (an alphaherpesvirus of

birds) and KSHV (a gammaherpesvirus of humans) encode similar mimics of miR-155, and Epstein-Barr virus (another gammaherpesvirus of humans) induces higher levels of host miR-155 in infected B cells (22, 23, 25, 26). A second important observation is that SFVagm-miR-S6-3p shares seed identity with the host miRNA family miR-132/212. KSHV induces host miR-132 during infection, and miR-132 suppresses innate immunity (27). In independent assays, we demonstrate that, similar to miR-132, miR-S6 can suppress IFN-induced responses (Fig. 5). These combined observations lead to the interesting hypothesis that the otherwise unrelated KSHV and SFVagm have evolved independently to tap into the same host miR-155 and miR-132 regulatory pathways.

FVs have been noted for having the longest LTRs of reported retroviruses (1). Previous reports indicate that SFVs passaged in cell culture have a propensity to undergo deletions of portions of the U3 region of the LTR (38, 39). Interestingly, these reported deletions are in the miRNA cluster region, and viruses with these deletions were shown to replicate better in fibroblast cell culture (38). These observations raise the possibility that, similar to what has been reported for polyoma and herpesviruses (10, 11, 40, 41), some of the FV miRNAs contribute to optimizing virus gene expression and/or the establishment of viral reservoirs and/or the switch from latent to productive infectious cycles. It has also been reported that an SFV is targeted by a cell type-specific host miRNA and also encodes the protein Tas, which functions both as the viral transactivator and as a proposed inhibitor of miRNAs (42). From this published work, one might hypothesize that Tas could function to negatively regulate viral miRNA activity to promote/enhance productive infection; however, this seems unlikely given that the miRNA-inhibitory function of Tas has failed to be independently reproduced by other laboratories (43). Future studies will be needed to directly address the roles of the miRNAs in virus replication.

While FVs are not currently associated with disease states either in nonhuman primate populations in which they are endemic or in zoonotic human infections, our findings suggest new associations to investigate. Exogenous expression of miR-155, as well as infection with herpesviruses that encode miR-155 analogs, has been associated with lymphoproliferative disease (37, 44). Whether any such disease association exists for SFVagm in its natural host or in zoonotically infected humans remains to be seen.

The discovery of FV miRNA genes in the LTR region may have applications to retroviral vector development. Vector designs should be reviewed for the unintended inclusion of viral miRNA genes. The importance of this is further emphasized since these viral miRNAs may function as analogs of some host immunosuppressive or oncogenic miRNAs. Fortunately, current-generation FV vectors typically exclude the FV U3 region that would contain the FV miRNAs in favor of other, chimeric sequences (45–47). Alternatively, the SFV miRNAs provide inspiration for new architectures of small RNA transgene delivery.

In summary, we have demonstrated that SFVs encode a cluster of viral miRNAs in their LTRs via unconventional biogenesis mechanisms. Some of these viral miRNAs mimic host miRNAs, including a host oncomiR, miR-155, and an innate immune suppressor, miR-132. These findings have important implications for understanding the biology of foamy viruses, zoonotic foamy infections, miRNA biogenesis, and the development of FVs as vectors.

MATERIALS AND METHODS

See Text S1 in the supplemental material for full details of materials and methods used in the study.

Cell lines. HeLa, HEK293, and HEK293T cell lines were obtained from American Type Culture Collection (ATCC) and maintained in Dulbecco modified Eagle medium (DMEM) supplemented with 10% (vol/vol) fetal bovine serum (FBS) and penicillin-streptomycin (Pen-Strep) (Cellgro). Dicer wild-type cells (DLD1) and cells hypomorphic for Dicer activity (DLD1 DicerEx5$^{-/-}$) (20) were maintained in RPMI 1640 supplemented with 10% (vol/vol) FBS and Pen-Strep. The human B-cell line GM19240 was obtained from the Coriell Institute and maintained in RPMI 1640 supplemented with 15% (vol/vol) FBS and Pen-Strep.

Plasmids. Plasmid constructs were generated with standard molecular cloning techniques. See Text S1 and Data Set S2 in the supplemental material for complete details and sequences.

Generation of stable cell lines expressing SFVagm-miR-S6S7 and controls. Lentiviral transduction of the GM19240 cell line and selection with puromycin were performed as previously described (30).

miRNA prediction software. Scripts and associated data will be made freely available at https://code.google.com/p/mirna/.

Small RNA Northern blots. Small RNA Northern blot analysis was performed as previously described (48). Band intensities were measured using Quantity One image analysis software (Bio-Rad). Probe sequences are listed in Data Set S2 in the supplemental material.

Preparation of FV stocks. SFVagm (SFV-HU1, ATCC VR-2596) was amplified by serial passage on BHK21 cells. SFVagm stock titers (syncytia-forming units per ml [SFU/ml]) were determined by serial dilution and infection of BHK21 cells followed by staining with 0.5% (wt/vol) methylene blue and 50% methanol (vol/vol) solution and counting of syncytia.

Small RNA sequencing. Fifty-percent confluent HeLa cells in a T75 flask were infected with 5.4×10^4 SFU of SFVagm. Seventy-two hours postinfection, total RNA was harvested with PIG-B (49). Two hundred micrograms of total RNA was size fractionated on a 15% (vol/vol) urea-PAGE gel and used to prepare pooled (45% of pooled RNA) small RNA libraries for Illumina small RNA sequencing. Sequencing was performed on an Illumina HiSeq 2500 at the Genomic Sequencing and Analysis Facility at the University of Texas, Austin. Postprocessing and analysis of sequence data were carried out as previously described (30).

Precursor miRNA structure prediction. miRNA stem-loop secondary structures were generated using the Mfold RNA folding prediction Web server (50, 51). RNAfold software was used in the miRNA prediction pipeline (52).

RISC activity assay. HEK293T cells were transfected and dual-luciferase reporter assays were performed as previously described (30).

RNA polymerase activity assay. HEK293T cells were transfected with miRNA expression vectors as indicated. Two hours later, the cells were treated with 50 μg/ml α-amanitin (Sigma-Aldrich). Total RNA was harvested with PIG-B (49) at 24 h posttransfection, and Northern blot analysis was performed.

Drosha siRNA assay. Small interfering RNA (siRNA) knockdown of Drosha was followed by transfection of miRNA expression vectors in HEK293T cells and then by Northern blot analysis as previously described (30).

Microprocessor overexpression. Sequential transfection of HEK293T cells with Drosha/DGCR8 vectors and miRNA expression vectors, followed by Northern blot analysis, were performed as previously described (15).

Drosha cleavage efficiency assay. Cotransfection of HEK293T cells with miRNA expression vectors and Drosha/DGCR8 vectors was performed as previously described (30).

Dicer dependence assay. Dicer wild-type cells (DLD1) and cells hypomorphic for Dicer activity (DLD1 DicerEx5$^{-/-}$) (20) were transfected with miRNA expression vectors using the TurboFect reagent (Fermentas).

Twenty-four hours posttransfection, total RNA was extracted with PIG-B and Northern blot analysis was performed.

Host target 3′ UTR luciferase assays. Fifty-percent-confluent HEK293T cells in 24-well plates were cotransfected with 0.5 ng of the indicated luciferase reporters (pGL3-based BACH1 reporters and empty-vector controls included cotransfection with pcDNA3.1dsLuc2CP control vector; psiCheck2-based p300 reporters express both firefly and *Renilla* luciferase from the same plasmid) and 0.5 μg of the indicated miRNA expression vectors using the TurboFect reagent (Fermentas) in triplicate. Twenty-four hours posttransfection, cells were harvested and assayed with the Dual-Glo luciferase assay system (Promega). Luciferase activity was measured with a Luminoskan Ascent luminometer (Thermo Electronic). Student's *t* test was used to assess the statistical significance of observed differences.

Western immunoblot analysis. Fifty-percent-confluent 6-well plates of HeLa cells were infected with 1.35×10^4 SFU of SFVagm or mock infected. Twenty-four hours later, the medium was replaced with fresh medium. Ninety-six hours after infection, lysates were prepared as previously described (30). Fifty micrograms of the total lysate was separated in NuPAGE 4 to 12% bis-Tris gels and transferred to nitrocellulose membranes (Bio-Rad). Membranes were blocked with Odyssey blocking buffer (Li-Cor). The primary antibodies used were p300 (C-20) (sc-585; Santa Cruz Biotechnology), BACH1 (C-20) (sc-14700; Santa Cruz Biotechnology), and β-actin (C4) (sc-47778; Santa Cruz Biotechnology). Blots were scanned on an Odyssey CLx infrared imaging system (Li-Cor). Band intensities were measured with Image Studio software (Li-Cor). Three independent experiments were performed on different days for quantification, and Student's *t* test was used to assess the statistical significance of observed differences.

Interferon signaling assay. HEK293T cells were seeded in 96-well plates. The next day, 5 ng pcDNA3.1dsRluc and 20 ng pISRE-Luc (Clonetech) were cotransfected along with 100 ng of the indicated miRNA expression vector or control vector using the TurboFect transfection reagent (Fermentas). The mixture for each experimental condition was transfected into 6 wells (2 sets of triplicates—3 control wells and 3 experimental wells). After 48 h, the medium was replaced with new medium with or without 100 U/ml of universal type I interferon (PBL Interferon Source). Twelve hours after the IFN treatment, a dual-luciferase assay was performed. Three independent experiments were performed, each in triplicate.

Interferon growth assay. Stable B-cell lines were treated with interferon, and cell viability was assayed by trypan blue staining as previously described (30). Three independent experiments were performed, each in triplicate.

SUPPLEMENTAL MATERIAL

Supplemental material for this article may be found at http://mbio.asm.org/lookup/suppl/doi:10.1128/mBio.00074-14/-/DCSupplemental.

Figure S1, TIF file, 1.4 MB.
Figure S2, TIF file, 0.6 MB.
Figure S3, TIF file, 0.4 MB.
Figure S4, TIF file, 0.5 MB.
Figure S5, TIF file, 0.3 MB.
Table S1, DOCX file, 0.1 MB.
Table S2, DOCX file, 0.1 MB.
Text S1, DOCX file, 0.1 MB.
Data Set S1, XLSX, 0.1 MB.
Data Set S2, XLSX, 0.1 MB.

ACKNOWLEDGMENTS

This work was supported by grants RO1AI077746 from the National Institutes of Health, RP110098 from the Cancer Prevention & Research Institute of Texas, a Burroughs Wellcome Investigators in Pathogenesis Award to C.S.S., a UT Austin Powers graduate fellowship to R.P.K., a UT Austin Institute for Cellular and Molecular Biology fellowship, and the University of Würzburg.

We thank Bert Vogelstein (Johns Hopkins) for the Dicer hypomorph cell lines, Rolf Renne (University of Florida) for BACH1 luciferase reporters, Dimitris Lagos (University of York) for p300 luciferase reporters, Stephen Trent (UT Austin) for use of equipment, and the members of the Sullivan laboratory for comments regarding the manuscript.

REFERENCES

1. **Rethwilm A, Lindemann D.** 2013. Foamy viruses, p 1613–1632. *In* Knipe D, Howley P, Cohen JI, Griffin DE, Lamb RA, Martin MA, Racaniello VR, Roizman B (ed), Fields virology, 6th ed. Lippincott Williams & Wilkins, Philadelphia, PA.
2. **Heneine W, Switzer WM, Sandstrom P, Brown J, Vedapuri S, Schable CA, Khan AS, Lerche NW, Schweizer M, Neumann-Haefelin D, Chapman LE, Folks TM.** 1998. Identification of a human population infected with simian foamy viruses. Nat. Med. **4:**403–407. http://dx.doi.org/10.1038/nm0498-403.
3. **Wolfe ND, Switzer WM, Carr JK, Bhullar VB, Shanmugam V, Tamoufe U, Prosser AT, Torimiro JN, Wright A, Mpoudi-Ngole E, McCutchan FE, Birx DL, Folks TM, Burke DS, Heneine W.** 2004. Naturally acquired simian retrovirus infections in Central African hunters. Lancet **363:**932–937. http://dx.doi.org/10.1016/S0140-6736(04)15787-5.
4. **Betsem E, Rua R, Tortevoye P, Froment A, Gessain A.** 2011. Frequent and recent human acquisition of simian foamy viruses through apes' bites in central Africa. PLoS Pathog. **7:**e1002306. http://dx.doi.org/10.1371/journal.ppat.1002306.
5. **Schweizer M, Falcone V, Gänge J, Turek R, Neumann-Haefelin D.** 1997. Simian foamy virus isolated from an accidentally infected human individual. J. Virol. **71:**4821–4824.
6. **Switzer WM, Bhullar V, Shanmugam V, Cong ME, Parekh B, Lerche NW, Yee JL, Ely JJ, Boneva R, Chapman LE, Folks TM, Heneine W.** 2004. Frequent simian foamy virus infection in persons occupationally exposed to nonhuman primates. J. Virol. **78:**2780–2789. http://dx.doi.org/10.1128/JVI.78.6.2780-2789.2004.
7. **Boneva RS, Switzer WM, Spira TJ, Bhullar VB, Shanmugam V, Cong ME, Lam L, Heneine W, Folks TM, Chapman LE.** 2007. Clinical and virological characterization of persistent human infection with simian foamy viruses. AIDS Res. Hum. Retroviruses **23:**1330–1337. http://dx.doi.org/10.1089/aid.2007.0104.
8. **Linial M.** 2000. Why aren't foamy viruses pathogenic? Trends Microbiol. **8:**284–289. http://dx.doi.org/10.1016/S0966-842X(00)01763-7.
9. **Rua R, Betsem E, Gessain A.** 2013. Viral latency in blood and saliva of simian foamy virus-infected humans. PLoS One **8:**e77072. http://dx.doi.org/10.1371/journal.pone.0077072.
10. **Grundhoff A, Sullivan CS.** 2011. Virus-encoded microRNAs. Virology **411:**325–343. http://dx.doi.org/10.1016/j.virol.2011.01.002.
11. **Kincaid RP, Sullivan CS.** 2012. Virus-encoded microRNAs: an overview and a look to the future. PLoS Pathog. **8:**e1003018. http://dx.doi.org/10.1371/journal.ppat.1003018.
12. **Cullen BR.** 2011. Viruses and microRNAs: RISCy interactions with serious consequences. Genes Dev. **25:**1881–1894. http://dx.doi.org/10.1101/gad.17352611.
13. **Skalsky RL, Cullen BR.** 2010. Viruses, microRNAs, and host interactions. Annu. Rev. Microbiol. **64:**123–141. http://dx.doi.org/10.1146/annurev.micro.112408.134243.
14. **Boss IW, Renne R.** 2010. Viral miRNAs: tools for immune evasion. Curr. Opin. Microbiol. **13:**540–545. http://dx.doi.org/10.1016/j.mib.2010.05.017.
15. **Kincaid RP, Burke JM, Sullivan CS.** 2012. RNA virus microRNA that mimics a B-cell oncomir. Proc. Natl. Acad. Sci. U. S. A. **109:**3077–3082. http://dx.doi.org/10.1073/pnas.1116107109.
16. **Lewis BP, Burge CB, Bartel DP.** 2005. Conserved seed pairing, often flanked by adenosines, indicates that thousands of human genes are microRNA targets. Cell **120:**15–20. http://dx.doi.org/10.1016/j.cell.2004.12.035.
17. **Bogerd HP, Karnowski HW, Cai X, Shin J, Pohlers M, Cullen BR.** 2010. A mammalian herpesvirus uses noncanonical expression and processing mechanisms to generate viral microRNAs. Mol. Cell **37:**135–142. http://dx.doi.org/10.1016/j.molcel.2009.12.016.
18. **Lee SI, Murthy SC, Trimble JJ, Desrosiers RC, Steitz JA.** 1988. Four novel U RNAs are encoded by a herpesvirus. Cell **54:**599–607. http://dx.doi.org/10.1016/S0092-8674(88)80004-7.

19. **Kim VN, Han J, Siomi MC.** 2009. Biogenesis of small RNAs in animals. Nat. Rev. Mol. Cell Biol. **10:**126–139. http://dx.doi.org/10.1038/nrm2632.
20. **Cummins JM, He Y, Leary RJ, Pagliarini R, Diaz LA, Sjoblom T, Barad O, Bentwich Z, Szafranska AE, Labourier E, Raymond CK, Roberts BS, Juhl H, Kinzler KW, Vogelstein B, Velculescu VE.** 2006. The colorectal microRNAome. Proc. Natl. Acad. Sci. U. S. A. **103:**3687–3692. http://dx.doi.org/10.1073/pnas.0511155103.
21. **McClure LV, Sullivan CS.** 2008. Kaposi's sarcoma herpes virus taps into a host microRNA regulatory network. Cell Host Microbe **3:**1–3. http://dx.doi.org/10.1016/j.chom.2007.12.002.
22. **Gottwein E, Mukherjee N, Sachse C, Frenzel C, Majoros WH, Chi JT, Braich R, Manoharan M, Soutschek J, Ohler U, Cullen BR.** 2007. A viral microRNA functions as an orthologue of cellular miR-155. Nature **450:**1096–1099. http://dx.doi.org/10.1038/nature05992.
23. **Zhao Y, Yao Y, Xu H, Lambeth L, Smith LP, Kgosana L, Wang X, Nair V.** 2009. A functional microRNA-155 ortholog encoded by the oncogenic Marek's disease virus. J. Virol. **83:**489–492. http://dx.doi.org/10.1128/JVI.01166-08.
24. **Cullen BR.** 2013. MicroRNAs as mediators of viral evasion of the immune system. Nat. Immunol. **14:**205–210. http://dx.doi.org/10.1038/ni.2537.
25. **Linnstaedt SD, Gottwein E, Skalsky RL, Luftig MA, Cullen BR.** 2010. Virally induced cellular microRNA miR-155 plays a key role in B-cell immortalization by Epstein-Barr virus. J. Virol. **84:**11670–11678. http://dx.doi.org/10.1128/JVI.01248-10.
26. **Skalsky RL, Samols MA, Plaisance KB, Boss IW, Riva A, Lopez MC, Baker HV, Renne R.** 2007. Kaposi's sarcoma-associated herpesvirus encodes an ortholog of miR-155. J. Virol. **81:**12836–12845. http://dx.doi.org/10.1128/JVI.01804-07.
27. **Lagos D, Pollara G, Henderson S, Gratrix F, Fabani M, Milne RS, Gotch F, Boshoff C.** 2010. miR-132 regulates antiviral innate immunity through suppression of the p300 transcriptional co-activator. Nat. Cell Biol. **12:**513–519. http://dx.doi.org/10.1038/ncb2054.
28. **Bhattacharya S, Eckner R, Grossman S, Oldread E, Arany Z, D'Andrea A, Livingston DM.** 1996. Cooperation of Stat2 and p300/CBP in signalling induced by interferon-alpha. Nature **383:**344–347. http://dx.doi.org/10.1038/383344a0.
29. **Yoshikawa T, Takata A, Otsuka M, Kishikawa T, Kojima K, Yoshida H, Koike K.** 2012. Silencing of microRNA-122 enhances interferon-alpha signaling in the liver through regulating SOCS3 promoter methylation. Sci. Rep. **2:**. http://dx.doi.org/10.1038/srep00637263.
30. **Kincaid RP, Burke JM, Cox JC, de Villiers E-M, Sullivan CS.** 2013. A human torque Teno virus encodes a microRNA that inhibits interferon signaling. PLoS Pathog. **9:**e1003818. http://dx.doi.org/10.1371/journal.ppat.1003818.
31. **Kozomara A, Griffiths-Jones S.** 2011. miRBase: integrating microRNA annotation and deep-sequencing data. Nucleic Acids Res. **39:**D152–D157.
32. **Rosewick N, Momont M, Durkin K, Takeda H, Caiment F, Cleuter Y, Vernin C, Mortreux F, Wattel E, Burny A, Georges M, Van den Broeke A.** 2013. Deep sequencing reveals abundant noncanonical retroviral microRNAs in B-cell leukemia/lymphoma. Proc. Natl. Acad. Sci. U. S. A. **110:**2306–2311. http://dx.doi.org/10.1073/pnas.1213842110.
33. **Zeng Y, Yi R, Cullen BR.** 2005. Recognition and cleavage of primary microRNA precursors by the nuclear processing enzyme Drosha. EMBO J. **24:**138–148. http://dx.doi.org/10.1038/sj.emboj.7600491.
34. **Han J, Lee Y, Yeom KH, Nam JW, Heo I, Rhee JK, Sohn SY, Cho Y, Zhang BT, Kim VN.** 2006. Molecular basis for the recognition of primary microRNAs by the Drosha-DGCR8 complex. Cell **125:**887–901. http://dx.doi.org/10.1016/j.cell.2006.03.043.
35. **Whisnant AW, Kehl T, Bao Q, Materniak M, Kuzmak J, Löchelt M, Cullen BR.** 12 February 2014. Identification of novel, highly expressed retroviral microRNAs in cells infected by bovine foamy virus. J. Virol. http://dx.doi.org/10.1128/JVI.03587-13.
36. **Eis PS, Tam W, Sun L, Chadburn A, Li Z, Gomez MF, Lund E, Dahlberg JE.** 2005. Accumulation of miR-155 and BIC RNA in human B cell lymphomas. Proc. Natl. Acad. Sci. U. S. A. **102:**3627–3632. http://dx.doi.org/10.1073/pnas.0500613102.
37. **Costinean S, Zanesi N, Pekarsky Y, Tili E, Volinia S, Heerema N, Croce CM.** 2006. Pre-B cell proliferation and lymphoblastic leukemia/high-grade lymphoma in Eμ-miR155 transgenic mice. Proc. Natl. Acad. Sci. U. S. A. **103:**7024–7029. http://dx.doi.org/10.1073/pnas.0602266103.
38. **Schmidt M, Herchenröder O, Heeney J, Rethwilm A.** 1997. Long terminal repeat U3 length polymorphism of human foamy virus. Virology **230:**167–178. http://dx.doi.org/10.1006/viro.1997.8463.
39. **De Celis-Kosmas J, Coronel A, Grigorian I, Emanoil-Ravier R, Tobaly-Tapiero J.** 1997. Non-random deletions in human foamy virus long terminal repeat during viral infection. Arch. Virol. **142:**1237–1246. http://dx.doi.org/10.1007/s007050050155.
40. **Umbach JL, Kramer MF, Jurak I, Karnowski HW, Coen DM, Cullen BR.** 2008. MicroRNAs expressed by herpes simplex virus 1 during latent infection regulate viral mRNAs. Nature **454:**780–783.
41. **Broekema NM, Imperiale MJ.** 2013. miRNA regulation of BK polyomavirus replication during early infection. Proc. Natl. Acad. Sci. U. S. A. **110:**8200–8205. http://dx.doi.org/10.1073/pnas.1301907110.
42. **Lecellier CH, Dunoyer P, Arar K, Lehmann-Che J, Eyquem S, Himber C, Saïb A, Voinnet O.** 2005. A cellular microRNA mediates antiviral defense in human cells. Science **308:**557–560. http://dx.doi.org/10.1126/science.1108784.
43. **Lin J, Cullen BR.** 2007. Analysis of the interaction of primate retroviruses with the human RNA interference machinery. J. Virol. **81:**12218–12226. http://dx.doi.org/10.1128/JVI.01390-07.
44. **Zhao Y, Xu H, Yao Y, Smith LP, Kgosana L, Green J, Petherbridge L, Baigent SJ, Nair V.** 2011. Critical role of the virus-encoded microRNA-155 ortholog in the induction of Marek's disease lymphomas. PLoS Pathog. **7:**e1001305. http://dx.doi.org/10.1371/journal.ppat.1001305.
45. **Lindemann D, Rethwilm A.** 2011. Foamy virus biology and its application for vector development. Viruses **3:**561–585. http://dx.doi.org/10.3390/v3050561.
46. **Trobridge G, Vassilopoulos G, Josephson N, Russell DW.** 2002. Gene transfer with foamy virus vectors. Methods Enzymol. **346:**628–648.
47. **Heinkelein M, Dressler M, Jármy G, Rammling M, Imrich H, Thurow J, Lindemann D, Rethwilm A.** 2002. Improved primate foamy virus vectors and packaging constructs. J. Virol. **76:**3774–3783. http://dx.doi.org/10.1128/JVI.76.8.3774-3783.2002.
48. **McClure LV, Lin YT, Sullivan CS.** 2011. Detection of viral microRNAs by northern blot analysis. Methods Mol. Biol. **721:**153–171. http://dx.doi.org/10.1007/978-1-61779-037-9_9.
49. **Weber K, Bolander ME, Sarkar G.** 1998. PIG-B: a homemade monophasic cocktail for the extraction of RNA. Mol. Biotechnol. **9:**73–77. http://dx.doi.org/10.1007/BF02752699.
50. **Zuker M.** 2003. Mfold Web server for nucleic acid folding and hybridization prediction. Nucleic Acids Res. **31:**3406–3415. http://dx.doi.org/10.1093/nar/gkg595.
51. **Mathews DH, Sabina J, Zuker M, Turner DH.** 1999. Expanded sequence dependence of thermodynamic parameters improves prediction of RNA secondary structure. J. Mol. Biol. **288:**911–940. http://dx.doi.org/10.1006/jmbi.1999.2700.
52. **Hofacker IL, Fontana W, Stadler PF, Bonhoeffer LS, Tacker M, Schuster P.** 1994. Fast folding and comparison of RNA secondary structures. Monatsh. Chem. **125:**167–188. http://dx.doi.org/10.1007/BF00818163.